文章编号:1673-2049(2014)01-0001-15

On North American and Chinese Standards for Design of Cold-formed Steel C-section Compressive Members

ZHOU Xu-hong[1], YUAN Xiao-li[2], XU Lei[2],
LIU Yong-jian[3], LIU Jing-nan[2]

(1. School of Civil Engineering, Chongqing University, Chongqing 400045, China; 2. School of Civil and Environmental Engineering, University of Waterloo, Waterloo N2L 3G1, Ontario, Canada; 3. School of Highway, Chang'an University, Xi'an 710064, Shaanxi, China)

Abstract: Nominal axial compressive strengths of cold-formed steel C-sections evaluated by the North American standard CSA S136-07 and the Chinese standard GB 50018—2002 were investigated. The procedures of evaluating the nominal axial compressive strength associated with both standards were analyzed and compared. The study results show that discrepancies between the two standards are primarily resulted from the difference in evaluating the effective area subjected to local buckling. For the C-section compressive members, the flange effective width calculated by the Chinese standard is much smaller than that of the North American standard, whereas the web effective width evaluated by the North American standard is slightly less than that of the Chinese standard. For typical C-section wall studs, the difference on the nominal axial strength is primarily influenced by the flange and web width-to-thickness ratios. When the flange width-to-thickness ratio is not less than 17.8, the difference on the nominal axial compressive strength is dominated by the difference of flange effective width between the two standards and the nominal axial compressive strength evaluated by GB 50018—2002 is less than that of CSA S136-07; when the flange width-to-thickness ratio is less than 17.8, the difference on the nominal axial compressive strength is then primarily governed by the difference of web effective width between the two standards and the nominal axial compressive strength evaluated by GB 50018—2002 is slightly greater than that of CSA S136-07.

Key words: cold-formed steel; C-section member; nominal axial compressive strength; flexural buckling; lateral-torsional buckling; effective width; buckling coefficient

CLC number: TU375.4 **Document code**: A

Received date: 2013-11-28

Biography: ZHOU Xu-hong(1956-), male, professor, doctoral advisor, academician of CAE, PhD, E-mail: zhouxuhong@126.com.

北美规范与中国规范关于冷弯薄壁型钢 C 形截面受压构件设计的比较

周绪红[1]，苑小丽[2]，徐 磊[2]，刘永健[3]，刘競楠[2]

（1. 重庆大学 土木工程学院，重庆 400045；2. 滑铁卢大学 土木与环境工程学院，安大略 滑铁卢 N2L 3G1；
3. 长安大学 公路学院，陕西 西安 710064）

摘要：对比了北美规范 CSA S136-07 和中国规范 GB 50018—2002 中关于冷弯薄壁型钢 C 形截面轴压构件的名义轴压强度。首先介绍了北美规范和中国规范计算名义轴压强度的方法，然后针对控制构件名义轴压强度的 2 个主要参数，即屈曲应力和有效截面面积，对 2 本规范进行了深入对比，最后对典型 C 形墙架柱名义轴压强度进行了比较。研究结果表明：2 本规范具有相同的屈曲应力，但依据 2 本规范计算的有效截面面积却不同；一般来说，根据 GB 50018—2002 计算的翼缘有效宽度远小于根据 CSA S136-07 计算的结果，然而依据 CSA S136-07 计算的腹板有效宽度则略小于依据 GB 50018—2002 计算的结果；2 本规范名义轴压强度不同主要由 C 形截面翼缘和腹板有效宽厚比不同引起；当翼缘的宽厚比不小于 17.8 时，构件名义轴压强度的不同主要由翼缘有效宽厚比控制，根据 GB 50018—2002 计算的名义轴压强度小于根据 CSA S136-07 计算的结果；当翼缘的宽厚比小于 17.8 时，构件名义轴压强度的不同则主要受腹板有效宽度控制，依据 GB 50018—2002 计算的名义轴压强度略大于依据 CSA S136-07 计算的结果。

关键词：冷弯薄壁型钢；C 形截面构件；名义轴压强度；弯曲屈曲；弯扭屈曲；有效宽度；屈曲系数

0 Introduction

C-section is the most widely used section shape in cold-formed steel framing construction. A typical application of C-sections as compressive members is the load bearing wall studs. In North America, procedures of designing cold-formed steel members are specified in CSA S136-07[1]. In China, the design procedures of cold-formed steel members concerning with local buckling, flexural buckling and lateral-torsional buckling strength are stipulated in GB 50018—2002[2] while the procedure for evaluating the distortional buckling is specified in standard JGJ 227—2011[3]. Although theoretical basis for evaluating the compressive strength of cold-formed steel C-section members are similar in the North American and the Chinese standards, the differences still exist. The primary objectives of this study are to identify the differences between the standards CSA S136-07 and GB 50018—2002 on evaluating the nominal compressive strength of cold-formed steel C-section members and to investigate how the nominal compressive strength is affected by the differences.

In the paper, the procedures associated with the two standards for evaluating the nominal compressive strength of cold-formed steel C-section members are discussed. Then, two key parameters used for determining the nominal compressive strength of cold-formed steel members, the buckling stress and the associated effective width, are compared, respectively. Finally, the differences in the nominal axial compressive strength between the two standards are investigated for the typical C-section load bearing wall studs.

1 Expression of Nominal Axial Compressive Strength

C-section members is shown in Fig. 1. In Fig. 1, w_w is flat portion of the web; w_f is flat portion of the flange; b_0 is the outer-to-outer dimension of the flange; h_0 is outer-to-outer depth of the C-section members; x_0 is the distance from shear center to centroid along principal axis; d is flat portion of the stiffener; D is height of the stiffener; R is inside bend radius; r is centerline bend radius. Assumptions made for the comparisons on the nominal axial compressive strength of C-section members shown in Fig. 1 are as follows: ① the axial compressive load is applied through the centroid of the C-section members; ② there are no holes in the C-section members; ③ distortional buckling is

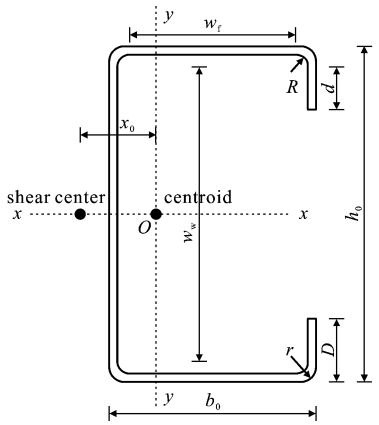

Fig. 1　Profile of C-section Member

图 1　C 形截面构件剖面

not considered; ④ the yield stress f_y of the steel is either $f_y = 345$ MPa or $f_y = 235$ MPa. In CSA S136-07, the equation to calculate the nominal axial strength P_n of a compressive member is

$$P_n = f_n A_e \tag{1}$$

where f_n is the nominal stress calculated based on the flexural and lateral-torsional buckling[4-6]; A_e is the effective area associated with the nominal stress f_n.

On the other hand, in GB 50018—2002, although the nominal axial strength P_n is not explicitly expressed, the standard provides the following equation to check member stability as

$$\frac{N}{\varphi A_e} \leqslant f \tag{2}$$

where N is the factored load; f is the design strength; φ is the stability coefficient; A_e is the effective area calculated at the stress φf.

To obtain the equivalent nominal axial strength P_n based on GB 50018—2002, Eq. (2) can be rewritten as

$$P_n = \varphi f_y A_e \tag{3}$$

Because the stability coefficient φ is a stress reduction factor which accounts for the flexural and lateral-torsional buckling of the compressive member, the products of φ and f_y in Eq. (3) can be considered as the equivalent to the nominal stress f_n in Eq. (1) as both of them are stresses calculated based on the flexural and lateral-torsional buckling.

Comparing Eq. (1) to Eq. (3), it can be seen that the two standards are similar while calculating the nominal compressive strength with an expression of the strength in terms of the product of the nominal stress f_n (or φf_y) and the effective area A_e. The nominal stress f_n or φf_y is evaluated based on the flexural and lateral-torsional buckling, and the effective area A_e is obtained with the consideration of the local buckling at the stress levels f_n or φf. In order to compare the nominal compressive strengths P_n between the two standards, the procedures of evaluating the flexural and lateral-torsional buckling stress and the effective area in each standard are needed to be investigated.

2　Flexural and Lateral-torsional Buckling Stress

In CSA S136-07, the nominal stress f_n is calculated as follows

$$f_n = \begin{cases} 0.658^{\lambda_c^2} f_y & \lambda_c \leqslant 1.5 \\ \dfrac{0.877}{\lambda_c^2} f_y & \lambda_c > 1.5 \end{cases} \tag{4}$$

where λ is slenderness factor, $\lambda = \sqrt{f_y / f_e}$, f_e is the least of the applicable elastic flexural buckling stress σ_e and flexural-torsional buckling stress σ_{ew}.

The stresses σ_e and σ_{ew} are defined as follows

$$\sigma_e = \frac{\pi^2 E}{(KL/r)^2} \tag{5}$$

$$\sigma_{ew} = \frac{1}{2\beta}\left[\sigma_{ex} + \sigma_t - \sqrt{(\sigma_{ex} + \sigma_t)^2 - 4\beta\sigma_{ex}\sigma_t}\right] \tag{6}$$

$$KL/r = \max\{K_x L_x / r_x, K_y L_y / r_y\} \tag{7}$$

where E is the elastic modulus, $E = 203$ GPa in CSA S136-07; KL/r is the maximum of the flexural slenderness ratios about the x and y axes; K_x and K_y, L_x and L_y, and r_x and r_y are effective length factors, unbraced lengths and radii of gyration of fully unreduced cross section about the x and y axes, respectively; σ_{ex} is the elastic flexural buckling stress about the x axis, $\sigma_{ex} = \pi^2 E / (K_x L_x / r_x)^2$; β is a parameter related with the geometry of the cross section.

β is evaluated as

$$\beta = 1 - (x_0 / r_0)^2 \tag{8}$$

where r_0 is the polar radius of gyration, $r_0 = \sqrt{r_x^2 + r_y^2 + x_0^2}$; σ_t is the elastic torsional buckling

stress.

σ_t is calculated as

$$\sigma_t=\frac{1}{Ar_0^2}[GJ+\frac{\pi^2 EC_w}{(K_tL_t)^2}] \tag{9}$$

where A is the gross area of the section; G is the shear modulus, $G=78$ GPa in CSA S136-07; C_w is the warping constant; J is torsional constant; K_t and L_t are the effective length factor and unbraced length for twisting, respectively.

In GB 50018—2002, tabulated values of the stability coefficient φ, which is equivalent to the ratio f_n/f_y in CSA S136-07, are listed in Appendix A based on the maximum slenderness ratio KL/r which is defined as

$$KL/r=\max\{K_xL_x/r_x, K_yL_y/r_y, (KL/r)_t\} \tag{10}$$

where $(KL/r)_t$ is equivalent lateral-torsional buckling slenderness ratio.

It is noted that the slenderness ratio KL/r in GB 50018—2002 (Eq. 10) is a little different from Eq. (7) defined in CSA S136-07. In CSA S136-07, KL/r is the maximum of the flexural buckling slenderness ratios K_xL_x/r_x and K_yL_y/r_y, whereas in GB 50018—2002, it is the maximum of the flexural buckling slenderness ratios K_xL_x/r_x, K_yL_y/r_y and the equivalent lateral-torsional buckling slenderness ratio $(KL/r)_t$. The equivalent lateral-torsional buckling slenderness ratio $(KL/r)_t$ is defined as

$$(KL/r)_t=\frac{K_xL_x}{r_x}\sqrt{\frac{s^2+i_0^2}{2s^2}+\sqrt{(\frac{s^2+i_0^2}{2s^2})^2-\frac{i_0^2-x_0^2}{s^2}}} \tag{11}$$

$$s^2=\frac{(K_xL_x/r_x)^2}{A}\sqrt{\frac{C_w}{L_t^2}+0.039G} \tag{12}$$

$$i_0^2=(\frac{K_xL_x}{r_x})^2+(\frac{K_yL_y}{r_y})^2+x_0^2 \tag{13}$$

If the equivalent lateral-torsional buckling slenderness ratio $(KL/r)_t$ in Eq. (11) is substituted into Eq. (5), which is used to calculate the elastic flexural buckling stress σ_e, the resulting equation will be the same as Eq. (6). Since Eq. (6) is used to evaluate the elastic lateral-torsional buckling stress σ_{ew} in CSA S136-07, it can be concluded that the equivalent lateral-torsional buckling slenderness ratio $(KL/r)_t$ in GB 50018—2002 can also be used to calculate the elastic lateral-torsional buckling stress σ_{ew} in CSA S136-07. Therefore, in the following comparisons, the slenderness ratio KL/r is the maximum of the flexural slenderness ratios K_xL_x/r_x, K_yL_y/r_y and the equivalent lateral-torsional buckling slenderness ratio $(KL/r)_t$. In addition, the nominal stress f_n in CSA S136-07 is only calculated based on the elastic flexural buckling stress σ_e in Eq. (5). Furthermore, the value of the stability coefficient φ is obtained from Appendix A of GB 50018—2002 based on the given value of KL/r.

The stability coefficient φ from Appendix A of GB 50018—2002 and ratio f_n/f_y calculated based on CSA S136-07 for steel with yield stress $f_y=345$ MPa and $f_y=235$ MPa are presented in Fig. 2. As it can be seen from Fig. 2, the differences between the stability coefficient φ and ratio f_n/f_y for both $f_y=345$ MPa and $f_y=235$ MPa steel are not significant. For steel with $f_y=345$ MPa and $f_y=235$ MPa, the differences of stability coefficient φ in GB 50018—2002 and ratio f_n/f_y of CSA S136-07 range from -3% to 5% and -9% to 0%, respectively. Therefore, it is concluded that the factored stress φf_y in GB 50018—2002 and the nominal strength f_n in CSA S136-07 can be considered as equivalent.

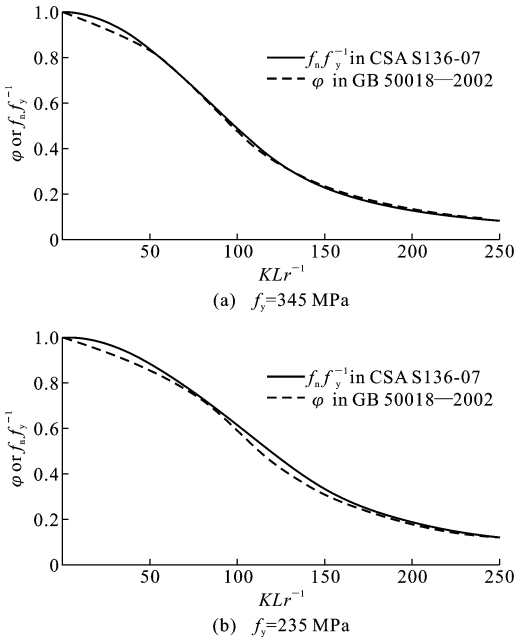

Fig. 2 Comparisons of Buckling Stresses

图 2 屈曲应力的比较

3 Procedure of Element Effective Width Evaluation

Since the procedures of evaluating the effective width of the cross-sectional elements in the two standards are different, it is not convenient to compare them directly. Therefore, the procedure described in GB 50018—2002 is rewritten equivalently to make the procedures of the two standards to be consistent and comparable. The comparison of the effective width calculation procedure in CSA S136-07 and the rewritten effective width calculation procedure in GB 50018—2002 is shown in Tab. 1. Since the different notations are used to express the dimensions of the C-section, the dimensional notations are redefined as shown in Fig. 1 for the reason of clarity. According to Tab. 1, both standards have the similarity of calculating the effective width based on the actual width-to-thickness ratio of the flat portion w/t, the plate buckling coefficient k, and the maximum stress σ_{max} of the considered element. However, the differences still exist. The primary differences between the two standards on evaluating the element effective width of the C-sections are:

(1) In step 1 shown in Tab. 1, the maximum stresses to calculate the local buckling σ_{max} defined in the two standards are different. In CSA S136-07, the maximum stress for compressive members $\sigma_{max}=f_n$, whereas in GB 50018—2002, $\sigma_{max}=\varphi f$. According to the requirement of GB 50018—2002, $f=300$ MPa for $f_y=345$ MPa and $f=205$ MPa for $f_y=235$ MPa. As discussed in section 2, since φ is basically the same as the ratio f_n/f_y, it is concluded that the maximum stress σ_{max} defined in GB 50018—2002 is approximately 87% of that specified in CSA S136-07.

表 1　Comparison of Calculation Procedure on Effective Width in CSA S136-07 and GB 50018—2002

Tab. 1　CSA S136-07 与 GB 50018—2002 中有效宽度计算过程的比较

Steps	CSA S136-07	GB 50018—2002
Step 1	Calculate the maximum stress σ_{max} and minimum stress σ_{min} for the considered element	Calculate the maximum stress σ_{max} and minimum stress σ_{min} for the considered element
Step 2	Determine the plate buckling coefficient k	Determine the plate buckling coefficient k and buckling coefficient related to the connected element k_1
Step 3	Calculate slenderness factor λ $\lambda=\frac{w}{t}\sqrt{\sigma_{max}\frac{12(1-\mu^2)}{k\pi^2E}}$	Calculate slenderness factor λ $\lambda=\frac{w}{t}\sqrt{\sigma_{max}\frac{12(1-\mu^2)}{kk_1\pi^2E}}$
Step 4	Evaluate local reduction factor ρ $\rho=\begin{cases}1 & \lambda\leqslant 0.673\\ (1-0.22/\lambda)/\lambda & \lambda>0.673\end{cases}$	Evaluate local reduction factor ρ $\rho=\begin{cases}1 & \lambda\leqslant 0.60\alpha\\ \sqrt{\frac{0.72\alpha}{\lambda}}-0.10 & 0.60\alpha<\lambda<1.26\alpha\\ 0.83\frac{\alpha}{\lambda} & \lambda\geqslant 1.26\alpha\end{cases}$ $\alpha=1.15-0.15\Psi\leqslant 1.15$, $\Psi=\frac{\sigma_{min}}{\sigma_{max}}$
Step 5	Calculate effective width b_e $b_e=\rho_w$	Calculate effective width b_e $b_e=\rho b_c$
Step 6	Distribute effective width	Distribute effective width

Note: As the two standards use different notations, the notations are redefined as follows (Fig. 1 and Fig. 4): b_c is compressed flat portion of the element; t is thickness; μ is Poisson ratio, $\mu=0.3$ for cold-formed steel; positive value for compressive stress; $E=203$ GPa in CSA S136-07, $E=206$ GPa in GB 50018—2002.

It is noted that in both standards, both the maximum stress σ_{max} and minimum stress σ_{min} for each element of the C-section, such as the web, flange and stiffener, are calculated based on the flexural and lateral-torsional buckling stresses of the member, not related to the actual applied load.

Since the maximum stresses specified in the two standards are different, to avoid confusion, the maximum stress σ_{max} in the following discussion

refers to the one defined in CSA S136-07 unless otherwise indicated.

(2) In step 2 and step 3, the influence of the support condition on the effective width of each element in CSA S136-07 is only represented by the plate buckling coefficient k. However, in GB 50018—2002, this influence is represented by the product of the plate buckling coefficient k and a modification coefficient k_1. The modification coefficient k_1 is introduced in GB 50018—2002 to explicitly account for the restraining effect of the connected element on the element under the consideration and it is calculated as

$$k_1=\begin{cases}0.11+\dfrac{0.93}{(\zeta-0.05)^2}\leqslant k_{1-\lim} & \zeta>1.1\\ \dfrac{1}{\sqrt{\zeta}}\leqslant k_{1-\lim} & \zeta\leqslant 1\end{cases} \tag{14}$$

$$\zeta=\frac{c}{b}\sqrt{\frac{k}{k_c}} \tag{15}$$

where c is the flat portion of the connected element; b is the flat portion of the element under the consideration; k and k_c are the buckling coefficients of the element under the consideration and the connected element; $k_{1-\lim}$ is the upper limit of k_1, $k_{1-\lim}=1.7$ for stiffened elements, $k_{1-\lim}=2.4$ for partially stiffened elements, and 3.0 for unstiffened elements.

Comparisons between the plate buckling coefficient k in CSA S136-07 and the product kk_1 in GB 50018—2002 for stiffener, flange, and web element of the compressive C-section members are discussed in section 4.

(3) In step 4, the local reduction factor ρ in CSA S136-07 is only associated with the slenderness factor λ. However, in GB 50018—2002, ρ is also related to the parameter α, a function of the stress distribution parameter Ψ as shown Tab. 1. As shown in Fig. 3(a), α ranges from 1 to 1.15: ① $\alpha=1$ when the element is subjected to uniform compressive stress ($\Psi=1$); ② $\alpha=1.15$ when the element is experienced to gradient compressive and tensile stress ($\Psi\leqslant 0$); ③ whereas the element is subjected to gradient compressive stress, α can be linearly interpolated by Ψ ($0<\Psi<1$).

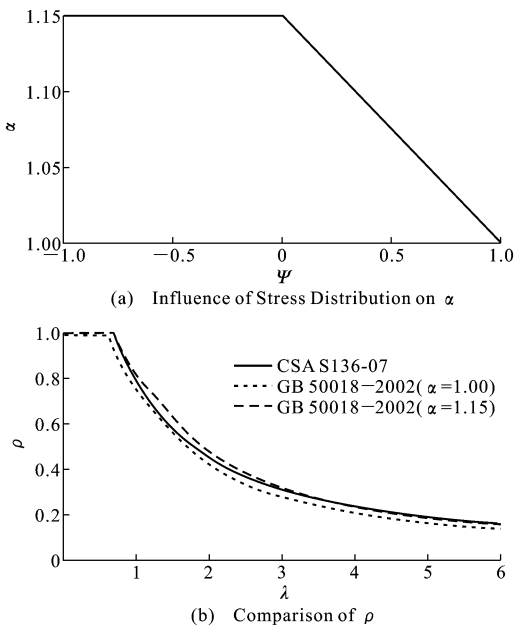

Fig. 3 Comparisons of Local Reduction Factor ρ

图 3 局部折减系数 ρ 的比较

The influence of α on the local reduction factor ρ in GB 50018—2002 is shown in Fig. 3(b). The local reduction factor ρ increases slightly with the increase of α. Although the two standards use different equations to calculate the local reduction factor ρ in step 4, the magnitude of the difference in the local reduction factor ρ is not significant: ① when $\alpha=1$, the local reduction factor ρ in GB 50018—2002 is slightly smaller than that in CSA S136-07; ② when $\alpha=1.15$, the local reduction factor ρ in GB 50018—2002 is slightly larger than that in CSA S136-07. Therefore, results obtained in step 4 in the two procedures can be considered as almost the same.

(4) In step 5, the effective width b_e is calculated based on the entire flat portion of the element w in CSA S136-07, whereas in GB 50018—2002, the effective width b_e is calculated based on the compressed flat portion of the element b_c (Fig. 4). However, for compressive members, since there is only compressive stress in the considered element, b_e and w are identical, as shown in Fig. 4(a). Therefore, step 5 in both standards for compressive member is considered the same.

(5) In step 6, the flange effective width distribution in CSA S136-07 for a compressive member

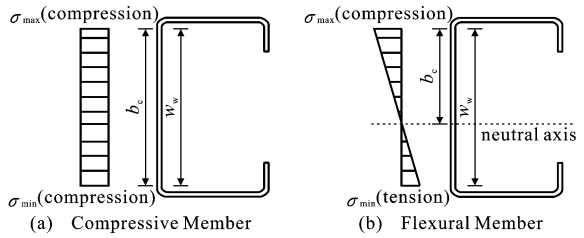

(a) Compressive Member　(b) Flexural Member

Fig. 4　Maximum and Minimum Stresses of C-section Member

图 4　C 形截面构件应力的最大值和最小值

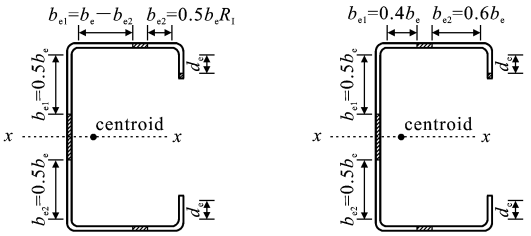

(a) CSA S136-07　(b) GB 50018—2002

Fig. 5　Comparison of Effective Width Distribution

图 5　有效宽度分布的比较

is different from that in GB 50018—2002. As shown in Fig. 5, for the flange of C-section, b_{e1} is effective width adjacent to the web whereas b_{e2} is the effective width adjacent to the stiffener. In CSA S136-07, $b_{e1}=b_e-b_{e2}$ and $b_{e2}=0.5b_eR_I$, whereas in GB 50018—2002, $b_{e1}=0.4b_e$ and $b_{e2}=0.6b_e$, as shown in Fig. 5. The parameter R_I is discussed in section 4.1. As $R_I\leqslant 1$, $b_{e1}\geqslant b_{e2}$ according to CSA S136-07, whereas based on GB 50018—2002, $b_{e1}<b_{e2}$. However, this difference has no influence on the total effective area and the nominal axial strength.

From the foregoing analysis, it can be concluded that the differences between the effective widths calculated by using CSA S136-07 and GB 50018—2002 are primarily resulted from: ① the difference in the determination of the maximum stress σ_{max}. The maximum stress σ_{max} in GB 50018—2002 is approximately 87% of that defined in CSA S136-07; ② the difference between the plate buckling coefficient k specified in CSA S136-07 and the product kk_1 defined in GB 50018—2002. The resulted differences between the effective widths evaluated based on CSA S136-07 and GB 50018—2002 for the stiffener, flange and web of C-sections in compressive member are discussed in section 4.

4　Element Effective Width of Compressive Member

4.1　Effective Width of Stiffener

The buckling coefficients of stiffener between the two standards are essentially identical being 0.425 and 0.43 for GB 50018—2002 and CSA S136-07, respectively. However, there is a considerable difference on how to evaluate the effective width of the stiffener between the two standards. The difference is primarily associated with the difference between coefficient k_{1L} defined in GB 50018—2002 and coefficient R_I specified in CSA S136-07 (Fig. 6). For $\frac{w_f/t}{S}\leqslant 0.328$, $b_e=w_f$, $b_{e1}=b_{e2}=w_f/2$, $R_I=1$, $d_e=d_e'$; for $\frac{w_f/t}{S}>0.328$, $R_I=\frac{I_s}{I_a}\leqslant 1$, $d_e=d_e'R_I$, $I_a=399t^4\left(\frac{w_f/t}{S}-0.328\right)^3\leqslant t^4\left(115\frac{w_f/t}{S}+5\right)$, $I_s=\frac{d^3t(\sin(\theta))^2}{12}$, $d=D-(R+t)$; $S=128\sqrt{E/\sigma_{max}}$, d_e is reduced effective width, d_e' is effective width of the stiffener calculated based on the unstiffened element. Buckling coefficient of flange k_f: for $D/w_f\leqslant 0.25$, $3.57R_I^n+0.43\leqslant 4$; for $0.25<D/w_f\leqslant 0.8$, $\left(4.82-5\frac{D}{w_f}\right)R_I^n+0.43\leqslant 4$; $n=0.582-\frac{w_f/t}{4S}\geqslant\frac{1}{3}$. The stiffener effective width d_e of CSA S136-07 is calculated as the products of the coefficient R_I and d_e', with d_e' being evaluated on the buckling coefficient k_L to consider the strength reduction effect caused by local buckling. The coefficient R_I is introduced to consider the effective width reduction caused the distortional buckling. If R_I is less than 1.0, distortional buckling may occur.

As shown in Fig. 7(a), the coefficient k_{1L} specified in GB 50018—2002 is associated with the ratio d/w_f between the flat portion of stiffener depth and the flat portion of flange width. The coefficient k_{1L} gradually increases from 0.18 to 0.95 as the ratio d/w_f increases from 0.18 to 0.6. On the other hand, R_I defined in CSA S136-07 is not

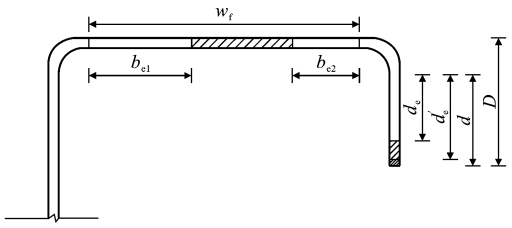

Fig. 6 Flange Buckling Coefficient k_f and Coefficient R_I in CSA S136-07

图 6 CSA S136-07 中的翼缘屈曲系数 k_f 与系数 R_I

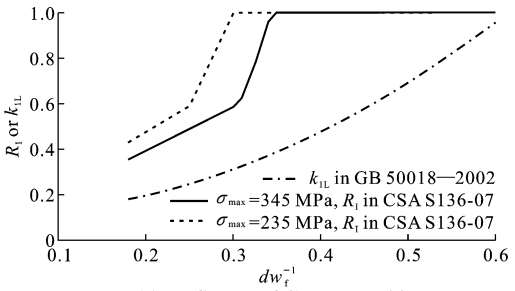

(a) Influence of d/w_f on R_I and k_{1L}

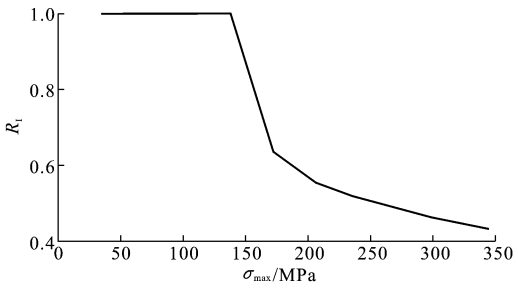

(b) Influence of σ_{max} on R_I (d/w_f=0.22)

Fig. 7 Plate Restraint Coefficient k_{1L} of Stiffener in GB 50018—2002 and Coefficient R_I in CSA S136-07 when d/t=9.5

图 7 d/t=9.5 时 GB 50018—2002 中的卷边板组约束系数 k_{1L} 与 CSA S136-07 中的系数 R_I

only associated with the ratio d/w_f but also related to the maximum stress σ_{max} as illustrated in Fig. 7. Generally, it is observed that: ① R_I increases with the increase of ratio d/w_f since distortional buckling normally occurs when the stiffener size is small [Fig. 7(a)]; ② R_I decreases with the increase of the maximum stress σ_{max} as lower magnitude of σ_{max} indicates the strength of the member is likely controlled by flexural or lateral-torsional buckling not the distortional buckling [Fig. 7(b)].

A demonstration of the stiffener effective width calculated based on the two standards is presented in Fig. 8 for a C-section with stiffener width-to-thickness ratio d/t = 9.5. As illustrated in Fig. 8(a), ratio d/w_f has significant influence on

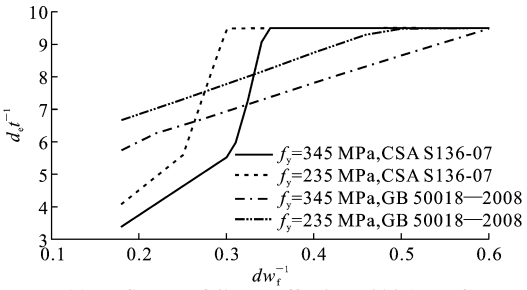

(a) Influence of d/w_f on Effective Width ($\sigma_{max}=f_y$)

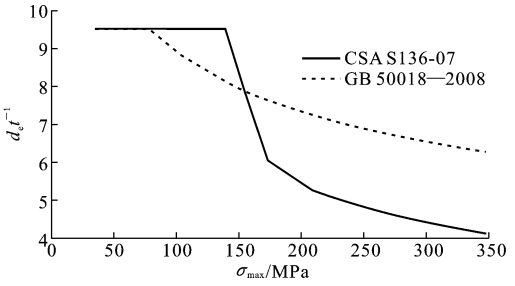

(b) Influence of σ_{max} on Effective Width (d/w_f=0.22)

Fig. 8 Comparisons of Stiffener Effective Widths when d/t=9.5

图 8 d/t=9.5 时卷边有效宽度的比较

the effective widths calculated based on the both two standards. For a stiffener with ratio d/t=9.5 and the maximum stress $\sigma_{max}=f_y$, the followings are observed:

(1) When ratio d/w_f is 0.18, although the coefficient k_{1L} of GB 50018—2002 is always less than the coefficient R_I of CSA S136-07 for both f_y=345 MPa and f_y=235 MPa steel as shown in Fig. 7(a), the stiffener effective width-to-thickness ratio d_e/t obtained from CSA S136-07 is less than that from GB 50018—2002. This is because coefficient R_I applies directly to effective width of the stiffener calculated based on the unstiffened element as discussed previously.

(2) With the increase of d/w_f, effective width-to-thickness d_e/t in CSA S136-07 increases rapidly due to the speedy increase of R_I shown in Fig. 7(a), whereas the increasing of d_e/t based on GB 50018—2002 is much less than that for both cases of f_y=345 MPa and f_y=235 MPa. Therefore, when ratio $d/w_f \geqslant 0.32$ for f_y=345 MPa and $d/w_f \geqslant 0.27$ for f_y=235 MPa in this case, the stiffener effective width-to-thickness ratio obtained from CSA S136-07 becomes greater than that from GB 50018—2002, as shown in Fig. 8(a).

(3) Eventually, with the further increase of d/w_f, the stiffener is fully effective based on both standards. In addition to the ratio d/w_f, the maximum stress σ_{max} also has considerable influence on the stiffener effective width. According to Fig. 8(b), for the cases of $d/t=9.5$ and $d/w_f=0.22$, the followings are perceived:

(1) When the magnitude of the maximum stress σ_{max} is small ($\sigma_{max}\leqslant 78$ MPa in this case), the stiffener is fully effective in accordance with both CSA S136-07 and GB 50018—2002.

(2) With the increase of σ_{max}, the stiffener is still fully effective based on CSA S136-07 as the value of R_I remains as 1.0 and ratio d_e/t associated with CSA S136-07 is greater than that of GB 50018—2002. However, the stiffener is not fully effective when $\sigma_{max}\geqslant 78$ MPa based on GB 50018—2002 due to the smaller value k_{1L}.

(3) With the further increase of σ_{max}, R_I begins to decrease rapidly as shown Fig. 7(b) whereas coefficient k_{1L} remains as a constant. Consequently, the stiffener effective width-to-thickness ratio d_e/t associated with CSA S136-07 becomes less than that of GB 50018—2002 when maximum stress $\sigma_{max}\geqslant 154$ MPa.

4.2 Effective Width of Flange

The plate buckling coefficients k_f of flange adopted in the two standards are quite different. In GB 50018—2002, the flange buckling coefficient is 0.98. However, in CSA S136-07, the flange buckling coefficient k_f is associated with the ratio d/w_f between flat portion of stiffener depth and flat portion of flange width, the ratio D/w_f of stiffener depth and the flat portion of flange width (assume the inside corner radius $R=2t$[7] which leads to $D=d+3t$), the maximum stress σ_{max} and the flange width-to-thickness ratio w_f/t as discussed in section 4.1 (Fig. 6). The influence of d/w_f and σ_{max} on the flange buckling coefficient k_f for the case when $w_f/t=45$ is demonstrated in Fig. 9(a). From Fig. 9(a), it can be seen that: ① when d/w_f is small ($d/w_f=0.21$ in this case), R_I is usually less than 1.0 ($R_I=0.41$ and $R_I=0.49$ for $f_y=345$ MPa and $f_y=235$ MPa in this case, respectively)

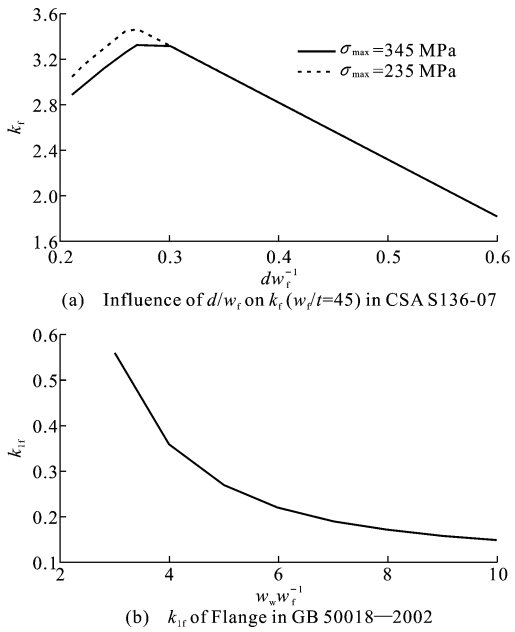

(a) Influence of d/w_f on k_f (w_f/t=45) in CSA S136-07

(b) k_{1f} of Flange in GB 50018—2002

Fig. 9 Flange Buckling Coefficient k_f in CSA S136-07 and k_{1f} of Flange Plate Restraint Coefficient in GB 50018—2002

图 9 CSA S136-07 中的翼缘屈曲系数 k_f 与 GB 50018—2002 中的翼缘板组约束系数 k_{1f}

as distortional buckling may occur; therefore, the resulted value of the flange buckling coefficient k_f is small ($k_f=2.98$ and $k_f=3.15$ for $f_y=345$ MPa and $f_y=235$ MPa, respectively); ② with the increase of d/w_f, the value k increases as the increase of value of R_I; ③ with further increase of ratio d/w_f, R_I reaches to 1.0 and distortional buckling will not occur. However, the stiffener becomes prone to the local buckling, and the flange buckling coefficient k_f decreases linearly with the increase of ratio d/w_f. Therefore, in order to stiffen the flange, the size of stiffener needs to be designed appropriately. Very large or small stiffeners may not be effective.

The maximum stress σ_{max} also has certain influence on the flange buckling coefficient k_f according to CSA S136-07. In the left side range of the peak amplitude of the coefficient k_f shown in Fig. 9(a), the increase in the flange buckling coefficient k_f is contributed by the increase of R_I shown in Fig. 7(a). Since R_I is associated with the maximum stress σ_{max} as shown in Fig. 7(b), therefore, the flange buckling coefficient k_f in that range is also associated with maximum stress σ_{max}. With the

increase of σ_{max}, the distortional buckling may occur; thus, the flange buckling coefficient k_f decreases as shown in Fig. 9(a).

Although the flange buckling coefficient k_f in CSA S136-07 is greatly influenced by d/w_f, for common C-sections with sizes of stiffener and flange satisfied requirements in both standards shown in Tab. 2, the influence of the different flange buckling coefficients on the flange effective width is small as illustrated in Fig. 10(a). The lines denoted as the maximum and minimum values shown in Fig. 10(a) respectively represent the maximum and minimum values of the flange local reduction factors ρ for various d/w_f corresponding to the values d/t shown in Tab. 2. It can be seen from Fig. 10(a), for given values of the width-to-thickness ratio w_f/t and the maximum stress σ_{max}, the variation of the flange local reduction factor is relatively small. This is because for C-sections satisfied requirements listed in Tab. 2, the stiffener sizes can effectively stiffen the flange to ensure that the local buckling of the flange occurs prior to the buckling of the stiffeners.

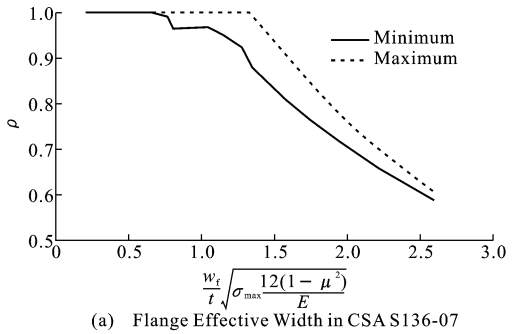

(a) Flange Effective Width in CSA S136-07

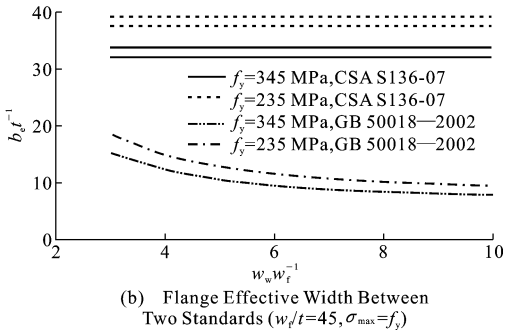

(b) Flange Effective Width Between Two Standards (w_f/t=45, $\sigma_{max}=f_y$)

Fig. 10 Comparisons of Flange Effective Widths

图 10 翼缘有效宽度的比较

A relationship of the flange effective width evaluated based on the two standards is illustrated in Fig. 10(b) for a case of $w_f/t=45$ and $\sigma_{max}=f_y$. It is observed from Fig. 10(b) that:

Tab. 2 Maximum and Minimum Stiffener Sizes for Flange

表 2 翼缘加劲肋的最大尺寸和最小尺寸

$w_f t^{-1}$		15	20	25	30	35	40	45	50	55	60
dt^{-1}	Maximum	9	12	12	12	12	12	12	12	12	12
	Minimum	5.4	6.3	7.2	8.0	8.5	9.0	9.5	10.0	10.5	11.0

(1) As the effective width-to-thickness ratio b_e/t of the flange in CSA S136-07 is not only associated with w_f/t and σ_{max}, but also the value of d/w_f, the two lines are used to describe the effective ratio b_e/t for each specified value of f_y. The upper and lower lines represent the maximum and minimum effective ratios b_e/t for various d/w_f, respectively.

Based on Tab. 2, for $w_f/t=45$, the associated maximum and minimum values of ratio d/t are 12 and 9.5, respectively. The resulted maximum and minimum values of $d/w_f=0.27$ and $d/w_f=0.21$ correspondingly, which are close to each other in this case. Therefore, the effective width-to-thickness ratio b_e/t of the flange in CSA S136-07 is not much influenced by d/w_f. b_e/t ranges from 31.2 to 33.8 for $f_y=345$ MPa and 37.2 to 39.2 for $f_y=235$ MPa.

(2) The effective width of the flange evaluated based on GB 50018—2002 is considerably less than that of CSA S136-07 due to the smaller value of product $k_f k_{1f}$ in GB 50018—2002. For the common C-sections, when $w_f/t=45$ and $\sigma_{max}=f_y$, the flange buckling coefficient k_f in CSA S136-07 ranges from 3.0 to 3.4 for $f_y=345$ MPa and 3.1 to 3.6 for $f_y=235$ MPa. However, the flange buckling coefficient k_f is only 0.98 in GB 50018—2002. Moreover, the flange buckling coefficient k_{1f} which is associated with the connected element in GB 50018—2002 is also much smaller than 1.0 as shown in Fig. 9(b). Therefore, the flange buckling coefficient k_f evaluated by CSA S136-07 is much larger than the coefficient $k_f k_{1f}$ specified in GB 50018—2002.

(3) Since coefficient k_{1f} is associated with the ratio w_w/w_f, from Fig. 9(b), k_{1f} of flange in GB 50018—2002 decreases from 0.56 to 0.15

when w_w/w_f increases from 3 to 10. Therefore, the differences in the flange effective widths between the two standards gradually become larger as the increase of w_w/w_f, as shown in Fig. 10(b). When ratio w_w/w_f increases from 3 to 10, the differences in the flange effective width between the two standards increase from 54.6% to 76.7% and 52.7% to 75.6% for $f_y=345$ MPa and $f_y=235$ MPa steel, respectively.

For C-sections satisfied with the requirements in both standards shown in Tab. 2, the flange buckling coefficient k_f calculated as per CSA S136-07 is in the range of 1.25 to 4.0. Therefore, it is concluded that for all C-sections satisfied with the requirements listed in Tab. 2, the flange buckling coefficient k_f evaluated based on CSA S136-07 is much larger than the coefficient k_fk_{1f} specified in GB 50018—2002, which results the effective width of the flange associated with GB 50018—2002 is much smaller than that of CSA S136-07.

4.3 Effective Width of Web

There is no difference on plate buckling coefficient k_w of the web of a C-section between the two standards: both of them specify 4.0 as the web buckling coefficient. The primary difference in the effective width comes from plate buckling coefficient k_{1w} related to the connected element. As shown in Fig. 11, coefficient k_{1w} for the web defined in GB 50018—2002 is associated with the ratio w_w/w_f. For C-sections with ratio w_w/w_f ranging from 3.0 to 10.0, coefficient k_{1w} increases from 1.22 to 1.7 when w_w/w_f increases from 3.0 to 6.0, and after that it remains as a constant of 1.7. For the web of C-sections, due to the large value of k_{1w}, the products of k_w and k_{1w} (k_wk_{1w}) in GB 50018—2002 is larger than the value k_w evaluated based on CSA S136-07. In addition, as the maximum stress σ_{max} in GB 50018—2002 is only 87% of the maximum stress σ_{max} specified in CSA S136-07, the effective width of the web in GB 50018—2002 is usually slightly greater than that in CSA S136-07 as shown Fig. 12. For a case of $w_w/t=120$ and $\sigma_{max}=f_y$: the effective width-to-thickness ratio of web is 42.2 and 50.2 for $f_y=345$ MPa and $f_y=235$ MPa steel in CSA S136-07, respectively, whereas in GB 50018—2002, the effective width-to-thickness ratio of web gradually increases from 45.6 to 53.9 for $f_y=345$ MPa and 55.2 to 65.2 for $f_y=235$ MPa when w_w/w_f increases from 3 to 6. When $w_w/w_f>6$, the effective width of web in GB 50018—2002 remains as a constant due to the upper limit $k_{1w}\leqslant 1.7$ for the web. For this case, the web effective width of GB 50018—2002 is 8.1% to 27.6% and 10.0% to 30.0% greater than that of CSA S136-07 for $f_y=345$ MPa and $f_y=235$ MPa steel, respectively.

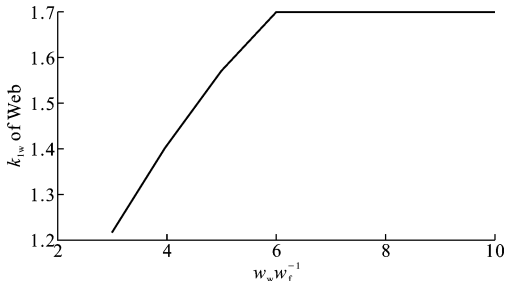

Fig. 11　Restraining Coefficient k_{1w} of Web in GB 50018—2002

图 11　GB 50018—2002 中的腹板板组约束系数 k_{1w}

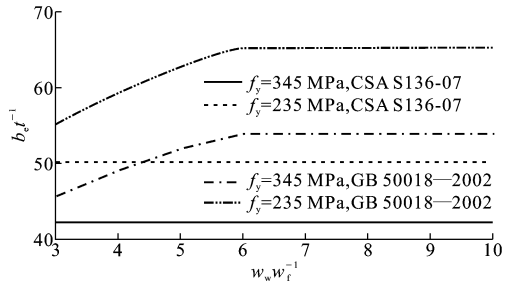

Fig. 12　Comparisons of Web Effective Widths when $w_w/t=120$, $\sigma_{max}=f_y$

图 12　$w_w/t=120$, $\sigma_{max}=f_y$ 时腹板有效宽度的比较

5 Comparison of Nominal Axial Compressive Strength

Two C-sections, with section thicknesses $t=2.58$ mm and $t=0.879$ mm as shown in Tab. 3 are selected from the *Handbook of Steel Construction*[8] for the nominal axial strength comparison in this study. The thicknesses $t=2.58$ mm and $t=0.879$ mm are likely the maximum and minimum thicknesses in load bearing wall stud application. The length of each member is 3.0 m and the weak

Tab. 3 Sizes of Members

表 3 构件尺寸

Member	Section Dimension/mm									Area/ mm^2	Length/ m	Bracing
	h_0	b_0	D	t	R	r	d	w_f	w_w			
A	152	41.3	12.7	2.580	3.87	5.16	6.25	28.40	139.10	621.32	3.0	2
B	152	41.3	12.7	0.879	1.94	2.38	9.88	35.66	146.36	221.86	3.0	2

Tab. 4 Comparison of Nominal Axial Compressive Strength

表 4 名义轴压强度的比较

Member	Standard	f_y=345 MPa			f_y=235 MPa		
		Stress f_n or φf_y/MPa	Effective Area A_e/mm^2	Nominal Axial Strength P_n/kN	Stress f_n or φf_y/MPa	Effective Area A_e/mm^2	Nominal Axial Strength P_n/kN
A	CSA S136-07	235.96	549.19	129.58	181.42	575.93	104.49
	GB 50018—2002	238.32	573.06	136.57	179.07	610.24	109.27
	Difference/%	1.0	4.3	5.4	−1.3	6.0	4.6
B	CSA S136-07	241.41	125.12	30.21	184.27	137.08	25.26
	GB 50018—2002	244.03	92.39	22.55	181.68	104.02	18.90
	Difference/%	1.1	−26.2	−25.4	−1.4	−24.1	−25.2

Tab. 5 Comparison of Effective Width when f_y=345 MPa

表 5 f_y=345 MPa 时有效宽度的比较

Member	Element	wt^{-1}	$b_e t^{-1}$			CSA S136-07		GB 50018—2002	
			CSA S136-07	GB 50018—2002	Difference/%	k	R_I	k	k_1
A	Web	53.91	43.08	48.62	12.9	4.00	N/A	4.00	1.56
	Flange	11.01	11.01	10.03	−8.9	N/A	N/A	0.98	0.27
	Stiffener	2.42	2.42	2.42	0.0	0.43	N/A	0.43	0.16
B	Web	166.51	51.12	58.67	14.8	4.00	N/A	4.00	1.43
	Flange	40.57	36.72	14.33	−61.0	3.37	N/A	0.98	0.35
	Stiffener	11.24	10.18	7.62	−25.1	0.43	0.89	0.43	0.24

Note: N/A means not applicable.

Tab. 6 Comparison of Effective Width when f_y=235 MPa

表 6 f_y=235 MPa 时有效宽度的比较

Member	Element	wt^{-1}	$b_e t^{-1}$			CSA S136-07		GB 50018—2002	
			CSA S136-07	GB 50018—2002	Difference/%	k	R_I	k	k_1
A	Web	53.91	47.10	52.58	11.6	4.00	N/A	4.00	1.56
	Flange	11.01	11.01	10.85	−1.5	N/A	N/A	0.98	0.27
	Stiffener	2.42	2.42	2.42	0.0	0.43	N/A	0.43	0.16
B	Web	166.51	57.85	67.89	17.4	4.00	N/A	4.00	1.43
	Flange	40.57	40.04	16.58	−58.6	3.47	N/A	0.98	0.35
	Stiffener	11.24	11.24	8.28	−26.3	0.43	1.00	0.43	0.24

axis of the member is braced at the 1/3 point and 2/3 point.

The comparisons on the buckling stress, effective cross-sectional area, nominal axial strength and the effective width for each member calculated in accordance with the two standards are presented in Tab. 4 to Tab. 6. It can be seen that the difference of the buckling stresses between the two standards is negligible as discussed in section 2. The difference in the nominal axial strength of the member is primarily resulted from the difference of the effective cross-sectional area.

For member A, since the actual width-to-thickness ratios w/t of the flange and the stiffener are small, flange and stiffener are both fully effective according to CSA S136-07, whereas in GB

50018—2002, although the flange is not fully effective, the effective widths are only 8.9 % and 1.5% less than those of CSA S136-07 for $f_y = 345$ MPa and $f_y = 235$ MPa steel. On the other hand, the web effective widths calculated based on GB 50018—2002 are 12.9% and 11.6% greater than those of CSA S136-07 for $f_y = 345$ MPa and $f_y = 235$ MPa steel as shown in Tab. 5 and Tab. 6. Therefore, there is no significant difference on the nominal axial strengths obtained from the two standards for this member. It can be seen from Tab. 4, the nominal axial strengths calculated based on GB 50018—2002 are about 5.4% and 4.6% greater than those evaluated based on CSA S136-07 for $f_y = 345$ MPa and $f_y = 235$ MPa steel, respectively.

However, for member B, the nominal axial strengths associated with GB 50018—2002 are 25.4% and 25.2% less than those of CSA S136-07 for $f_y = 345$ MPa and $f_y = 235$ MPa steel, respectively, as shown in Tab. 4. The smaller values of the nominal axial strength associated with GB 50018—2002 are primarily resulted from the smaller values of flange and stiffener effective widths. The flange effective widths calculated in accordance with GB 50018—2002 are 61.0% and 58.6% less than those of CSA S136-07 for $f_y = 345$ MPa and for $f_y = 235$ MPa steel, respectively, whereas the stiffener effective widths associated with GB 50018—2002 are 25.1% and 26.3% less than those of CSA S136-07 for $f_y = 345$ MPa and for $f_y = 235$ MPa steel, respectively, as shown in Tab. 5 and Tab. 6. Although the web effective widths calculated based on GB 50018—2002 are 14.8% and 17.4% respectively greater than those of CSA S136-07 for $f_y = 345$ MPa and for $f_y = 235$ MPa steel, it does not contribute significantly to the difference in the effective cross-sectional areas.

From the foregoing analysis, it can be seen the yield stress doesn't have significant influence on the difference of the nominal axial strength evaluated based on the two standards. The differences of the nominal axial strength between the two standards is greatly influenced by the cross-sectional dimensions of C-sections. Specifically, by comparing member A to member B, it is found that the difference on the nominal axial strength is primarily influenced by the flange width-to-thickness ratio w_f/t. For member A, as the flange width-to-thickness ratio is small ($w_f/t = 11.01$), the flange is almost fully effective in the both standards. The difference on the nominal axial strength is mainly controlled by the difference of the web effective width. Since the web effective width associated with GB 50018—2002 is usually greater than that of CSA S136-07 as discussed in section 4.3, the nominal axial strengths calculated based on GB 50018—2002 are about 5.4% and 4.6% greater than those evaluated based on CSA S136-07 for $f_y = 345$ MPa and $f_y = 235$ MPa steel, respectively, as shown in Tab. 4. However, for member B, the flange width-to-thickness ratio w_f/t is relatively large ($w_f/t = 40.57$). The difference on the nominal axial strength is primarily dominated by the difference of the flange effective width, whereas the difference of the web effective width doesn't have a significant contribution. Since the flange effective width associated with GB 50018—2002 is much less than that of CSA S136-07 as discussed in section 4.2, the nominal axial strengths associated with GB 50018—2002 are 25.4% and 25.2% less than those of CSA S136-07 for $f_y = 345$ MPa and $f_y = 235$ MPa steel, respectively, as shown in Tab. 4.

In order to further investigate effects of the flange width-to-thickness ratio w_f/t on the difference of the nominal axial strength between the two standards, comparisons of nominal axial strength between the two standards are carried out for typical C-section load-bearing wall studs with the section depth ranging from 92.1 mm to 203 mm. The first nineteen typical C-sections listed in Tab. 7 are selected from the *Handbook of Steel Construction*[8] and the rest are from the *Lightweight Steel Framing Metric Section Properties*[9]. The length of the stud is still assumed to be 3.0 m and the weak axis of the member is braced at the 1/3 point and 2/3 point. In addition, as the yield stress

Tab. 7 Comparison of Nominal Axial Compressive Strength for Typical C-section Wall Studs when f_y=345 MPa

表 7 f_y=345 MPa 时典型 C 形截面墙架柱名义轴压强度的比较

Member	Section Dimension/mm					$w_f t^{-1}$	$w_w w_f^{-1}$	P_n/kN		Difference/%
	h_0	b_0	D	t	R			CSA S136-07	GB 50018—2002	
1	203.0	63.4	19.10	2.580	3.87	19.57	3.76	200.07	190.86	−4.6
2	203.0	63.4	19.10	1.810	2.72	30.02	3.57	120.45	99.96	−17.0
3	203.0	63.4	19.10	1.440	2.16	39.03	3.48	85.48	64.56	−24.5
4	203.0	63.4	19.10	1.150	1.81	49.98	3.43	61.08	41.62	−31.9
5	203.0	50.8	19.10	2.580	3.87	14.69	5.02	174.32	179.08	2.7
6	203.0	50.8	19.10	1.810	2.72	23.06	4.65	109.77	97.84	−10.9
7	203.0	50.8	19.10	1.440	2.16	30.28	4.49	81.87	63.36	−22.6
8	203.0	50.8	19.10	1.150	1.81	39.03	4.39	56.62	41.31	−27.0
9	203.0	50.8	19.10	0.879	1.94	51.38	4.37	35.83	25.03	−30.1
10	203.0	41.3	12.70	2.580	3.87	11.01	6.69	130.03	141.60	8.9
11	203.0	41.3	12.70	1.810	2.72	17.81	6.02	81.29	84.53	4.0
12	203.0	41.3	12.70	1.440	2.16	23.68	5.74	60.13	55.40	−7.9
13	203.0	41.3	12.70	1.150	1.81	30.77	5.57	44.90	36.22	−19.3
14	203.0	41.3	12.70	0.879	1.94	40.57	5.53	30.18	22.33	−26.0
15	152.0	41.3	12.70	2.580	3.87	11.01	4.90	129.58	136.57	5.4
16	152.0	41.3	12.70	1.810	2.72	17.81	4.43	82.21	82.69	0.6
17	152.0	41.3	12.70	1.440	2.16	23.68	4.25	60.54	56.28	−7.0
18	152.0	41.3	12.70	1.150	1.81	30.77	4.13	45.08	36.68	−18.6
19	152.0	41.3	12.70	0.879	1.94	40.57	4.10	30.21	22.55	−25.4
20	152.0	50.8	15.90	2.580	3.87	14.69	3.67	154.59	155.16	0.4
21	152.0	50.8	15.90	1.810	2.72	23.06	3.42	97.46	91.58	−6.0
22	152.0	50.8	15.90	1.440	2.16	30.28	3.32	72.45	60.21	−16.9
23	152.0	50.8	15.90	1.150	1.81	39.03	3.25	51.75	39.31	−24.0
24	152.0	50.8	15.90	0.879	1.94	51.38	3.24	33.79	23.89	−29.3
25	101.6	41.3	12.70	2.580	3.87	11.01	3.13	92.87	91.44	−1.5
26	101.6	41.3	12.70	1.810	2.72	17.80	2.87	63.08	61.62	−2.3
27	101.6	41.3	12.70	1.440	2.16	23.67	2.77	47.17	44.14	−6.4
28	101.6	41.3	12.70	1.150	1.81	30.75	2.71	35.40	31.30	−11.6
29	101.6	41.3	12.70	0.879	1.94	40.55	2.69	25.06	19.90	−20.6
30	101.6	31.8	4.76	1.440	2.16	17.05	3.85	34.04	33.58	−1.4
31	101.6	31.8	4.76	1.150	1.81	22.46	3.70	24.32	23.68	−2.6
32	101.6	31.8	4.76	0.879	1.94	29.71	3.68	16.60	15.84	−4.6
33	92.1	41.3	12.70	2.580	3.87	11.01	2.79	79.44	77.61	−2.3
34	92.1	41.3	12.70	1.810	2.72	17.80	2.58	56.35	55.43	−1.6
35	92.1	41.3	12.70	1.440	2.16	23.67	2.49	42.48	40.00	−5.8
36	92.1	41.3	12.70	1.150	1.81	30.75	2.44	32.01	28.49	−11.0
37	92.1	41.3	12.70	0.879	1.94	40.55	2.43	22.87	18.97	−17.0
38	92.1	31.8	4.76	1.440	2.16	17.05	3.46	31.11	30.58	−1.7
39	92.1	31.8	4.76	1.150	1.81	22.46	3.34	22.33	21.58	−3.4
40	92.1	31.8	4.76	0.879	1.94	29.71	3.31	15.35	14.45	−5.8

doesn't have significant influence on the difference of the nominal axial strength, comparisons are only carried out for steel with f_y=345 MPa.

The differences of the nominal axial strength between the two standards are listed in Tab. 7 and are illustrated in Fig. 13. From Tab. 7, it is found that for given values of flange width-to-thickness ratio w_f/t, the ratio w_w/w_f has certain influence on

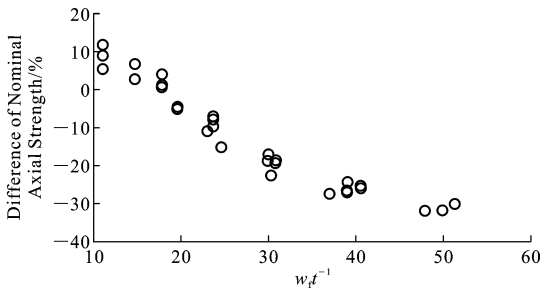

Fig. 13　Comparison of Nominal Axial Compressive Strength for Typical C-section Wall Studs when f_y=345 MPa

图 13　f_y=345 MPa 时典型 C 形截面墙架柱名义轴压强度的比较

the difference of the nominal axial strength, especially when the flange width-to-thickness ratio w_f/t is small. For example, for $w_f/t=11.1$, as ratio w_w/w_f increases from 2.79 to 6.69, the difference of the nominal axial strength between the two standards increases from −2.3% to 8.9%. This is because the difference of the web effective width between the two standards increases when w_w/w_f increases, as discussed in section 4.3.

However, it can be seen from Fig. 13 compared to the influence of w_w/w_f, the influence of the flange width-to-thickness ratio w_f/t is far more significant. The difference of the nominal axial strength between the two standards generally decreases with the increase of flange width-to-thickness ratio w_f/t. Approximately, if the flange width-to-thickness ratio w_f/t is not less than 17.8, the difference on the nominal axial strength is dominated by the difference of the flange effective width and the nominal axial strength evaluated by GB 50018—2002 is less than that of CSA S136-07, with the maximum difference being 31.9%. However, for the case that w_f/t is approximately less than 17.8, the difference on the nominal axial strength is dominated by the difference of the web effective width and the nominal axial strength evaluated by GB 50018—2002 is generally slightly greater than that of CSA S136-07, with the maximum magnitude being 8.9%.

6　Conclusions

The differences on evaluating the nominal axial compressive strength of cold-formed steel C-section based on the North American standard CSA S136-07 and the Chinese standard GB 50018—2002 are investigated. The investigation unveils that the differences are primarily resulted from the difference in computing the effective cross-sectional area at the specified buckling stresses. More specifically, it is contributed mainly from using different flange buckling coefficients and the maximum stress while evaluating the effective widths of the cross-section. The maximum stress σ_{max} used in GB 50018—2002 is approximately 87% of that used in CSA S136-07. However, it is also found in this study that the difference between the two standards in evaluating the flexural and lateral-torsional buckling stresses is negligible. The conclusions are obtained as follows:

(1) The flange effective width calculated based on the North American standard CSA S136-07 is considerably greater than that evaluated in Chinese standard GB 50018—2002. This is because GB 50018—2002 adopts smaller values of the flange buckling coefficients k_f and k_{1f}. In GB 50018—2002, the flange buckling coefficient k_f=0.98 and k_{1f} is usually less than 1.0. As a result, the products of k_f and k_{1f}($k_f k_{1f}$) in GB 50018—2002 is practically less than 1.0. On the contrast, the flange buckling coefficient k_f in CSA S136-07 normally ranges from 1.25 to 4.0.

(2) The web effective width calculated based on the Chinese standard is slightly greater than that computed from the North American standard. This is because the web buckling coefficient associated with the connected element k_{1w} is usually larger than 1.0 and the maximum stress σ_{max} in GB 50018—2002 is approximately 87% of that in CSA S136-07.

(3) The difference of the stiffener effective width between the two standards is a little bit complicated than that of the flange or web effective width. Generally, when the stiffener is small, the stiffener effective width calculated in CSA S136-07 may be less than that of GB 50018—2002. However, if the size of stiffener is large, the effective width

(下转第 55 页)

search，2002，46(4)：239-247.

[5] NAAR H，KUJALA P，SIMONSEN B C，et al. Comparison of the Crashworthiness of Various Bottom and Side Structures[J]. Marine Structures，2002，15(4/5)：443-460.

[6] PEDERSEN P T. Ship Impacts：Bow Collisions[J]. International Journal of Impact Engineerin，1993，13(2)：163-187.

[7] **高　震，顾永宁，胡志强. 结构冲击试验的校准计算[J]. 船舶力学**，2005，9(2)：77-82.
GAO Zhen，GU Yong-ning，HU Zhi-qiang. Benchmark Study of Structural Impact Test[J]. Journal of Ship Mechanincs，2005，9(2)：77-82.

[8] **李　军. 冲击数值模拟可靠性的试验检验[D]. 上海：同济大学**，2009.
LI Jun. Experimental Examination of the Trustworthiness of Impact Numerical Simulation[D]. Shanghai：Tongji University，2009.

[9] COWPER G R，Symonds P S. Strain Hardening and Strain Rate Effects in the Impact Loading of Cantilever Beams[R]. Providence：Brown University，1958.

[10] **华南理工大学，东南大学，浙江大学，等. 地基与基础[M]. 2 版. 北京：中国建筑工业出版社**，1991.
South China University of Technology，Southest University，Zhejiang University，et al. Soils and Foundations[M]. 2nd ed. Beijing：China Architecture & Building Press，1991.

[11] HUANG N E，WU M C，LONG S R，et al. A Confidence Limit for the Empirical Mode Decomposition and Hilbert Spectral Analysis[J]. Proceedings of the Royal Society A，2003，459(2037)：2317-2345.

[12] HUANG N E，SHEN Z，LONG S R，et al. The Empirical Mode Decomposition and the Hilbert Spectrum for Nonlinear and Non-stationary Time Series Analysis[J]. Proceedings of the Royal Society A，1998，454(1971)：903-995.

（上接第 15 页）

associated with CSA S136-07 will be greater than that of GB 50018—2002.

（4）The difference of the nominal axial strength between the two standards is primarily influenced by the flange width-to-thickness ratio. For typical C-section wall studs investigated herein，the difference on the nominal axial strength is primarily influenced by the flange width-to-thickness ratio w_f/t. If the flange width-to-thickness ratio w_f/t is not less than 17.8，the difference on the nominal axial strength is dominated by the difference of flange effective width，and the nominal axial strength evaluated by GB 50018—2002 is less than that of CSA S136-07，with the maximum difference being 31.9%. However，when w_f/t is approximately less than 17.8，then the difference on the nominal axial strength is primarily governed by the difference of the web effective width and the nominal axial strength evaluated by GB 50018—2002 is slightly greater than that of CSA S136-07，with the maximum difference being 8.9%.

References：

[1] CSA S136-07，North American Specification for the Design of Cold-formed Steel Structural Members[S].

[2] GB 50018—2002，Technical Code of Cold-formed Thin-wall Steel Structures[S].

[3] JGJ 227—2011，Technical Specification for Low-rise Cold-formed Thin-wall Steel Buildings[S].

[4] CHEN J. Stability of Steel Structures：Theory and Design[M]. Beijing：Science Press，2008.

[5] YU W W，LABOUBE R A. Cold-formed Steel Design[M]. New York：John Wiley & Sons，2010.

[6] ZHOU X H，WANG S J. Stability Theory and Its Applications of Thin-walled Members[M]. Beijing：Science Press，2009.

[7] XU L. Advanced Structural Steel Design[R]. Waterloo：University of Waterloo，2012.

[8] Canadian Institute of Steel Construction. Handbook of Steel Construction[M]. 10th ed. Markham：Canadian Institute of Steel Construction，2010.

[9] Canadian Sheet Steel Building Institute (CSSBI). Lightweight Steel Frame Metric Section Properties[R]. Cambridge：Canadian Sheet Steel Building Institute，2011.